



[2-Chloro-3-nitro-5-(trifluoromethyl)phenyl](piperidin-1-yl)methanone: structural characterization of a side product in benzothiazinone synthesis

Tamira Eckhardt,^a Richard Goddard,^b Ines Rudolph,^a Adrian Richter,^a Christoph Lehmann,^a Peter Imming^a and Rüdiger W. Seidel^{a*}

Received 14 July 2020
Accepted 3 August 2020

^aInstitut für Pharmazie, Wolfgang-Langenbeck-Str. 4, 06120 Halle (Saale), Germany, and ^bMax-Planck-Institut für Kohlenforschung, Kaiser-Wilhelm-Platz 1, 45470 Mülheim an der Ruhr, Germany. *Correspondence e-mail: ruediger.seidel@pharmazie.uni-halle.de

Edited by L. Van Meervelt, Katholieke Universiteit Leuven, Belgium

Keywords: benzothiazinones; nitrobenzamides; anti-tuberculosis drugs; reaction mechanism; crystal structure.

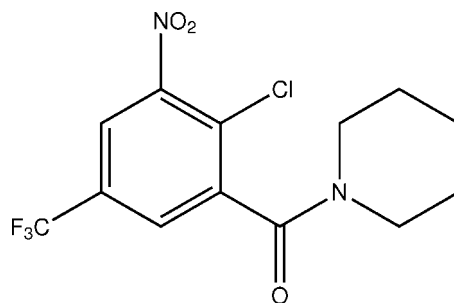
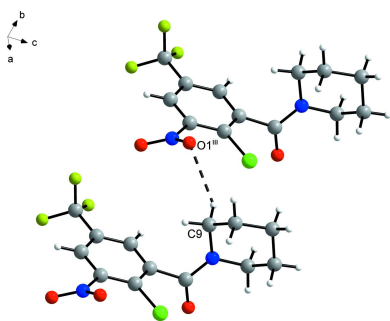
CCDC reference: 2021003

Supporting information: this article has supporting information at journals.iucr.org/e

1,3-Benzothiazin-4-ones (BTZs) are a promising new class of anti-tuberculosis drug candidates, some of which have reached clinical trials. The title compound, the benzamide derivative [2-chloro-3-nitro-5-(trifluoromethyl)phenyl](piperidin-1-yl)methanone, C₁₃H₁₂ClF₃N₂O₃, occurs as a side product as a result of competitive reaction pathways in the nucleophilic attack during the synthesis of the BTZ 8-nitro-2-(piperidin-1-yl)-6-(trifluoromethyl)-1,3-benzothiazin-4-one, following the original synthetic route, whereby the corresponding benzoyl isothiocyanate is reacted with piperidine as secondary amine. In the title compound, the nitro group and the nearly planar amide group are significantly twisted out of the plane of the benzene ring. The piperidine ring adopts a chair conformation. The trifluoromethyl group exhibits slight rotational disorder with a refined ratio of occupancies of 0.972 (2):0.028 (2). There is structural evidence for intermolecular weak C—H···O hydrogen bonds.

1. Chemical context

1,3-Benzothiazin-4-ones (BTZs) are promising anti-tuberculosis drug candidates, some of which have already reached clinical trials (Mikušová *et al.*, 2014; Makarov & Mikušová, 2020). Various methods for the synthesis of BTZs have been reported (Makarov *et al.*, 2007; Moellmann *et al.*, 2009; Makarov, 2011; Rudolph, 2014; Rudolph *et al.*, 2016; Zhang & Aldrich, 2019). In the original synthesis, 2-chlorobenzoyl chloride derivatives are reacted with ammonium or alkali metal thiocyanates to form the corresponding 2-chlorobenzoyl isothiocyanates (Makarov *et al.*, 2007; Moellmann *et al.*, 2009). These are reactive species and are treated *in situ* with secondary amines to afford the corresponding thiourea derivatives, which undergo ring closure to give 1,3-thiazin-4-ones *via* an intramolecular nucleophilic substitution reaction. The latter step is favoured when electron-withdrawing substituents are present on the benzene ring.



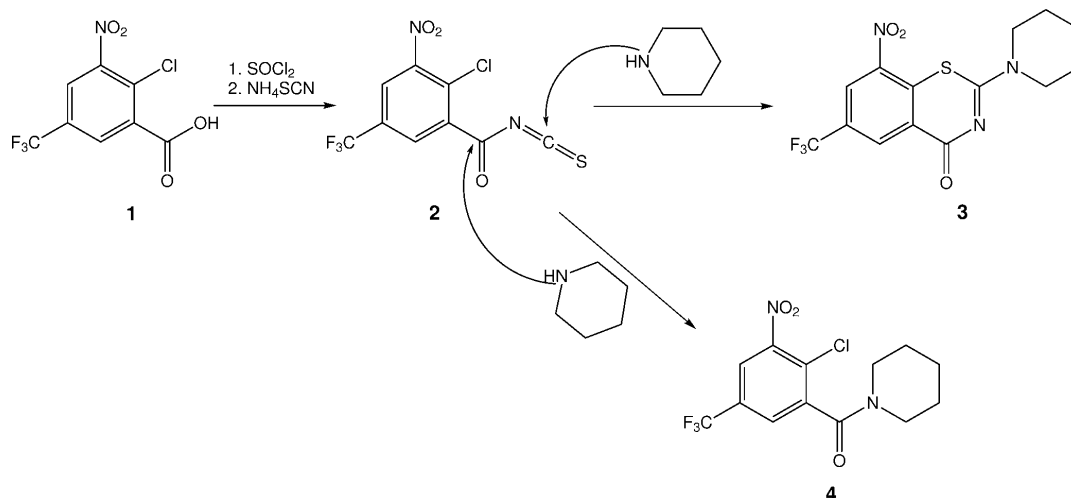


Figure 1

Synthetic pathway from 2-chloro-3-nitro-5-(trifluoromethyl)benzoic acid (**1**) to BTZ **3** and side product **4**, illustrating the two different points of nucleophilic attack of piperidine at the intermediate 2-chloro-3-nitro-5-(trifluoromethyl)benzoyl isothiocyanate (**2**), resulting in **3** and **4** (Rudolph, 2014).

Fig. 1 depicts the synthesis following the original procedure for a BTZ previously reported by us (Rudolph, 2014; Rudolph *et al.*, 2016; Richter, Rudolph *et al.*, 2018). After treatment of 2-chloro-3-nitro-5-(trifluoromethyl)benzoic acid (**1**) with thionyl chloride and subsequently ammonium thiocyanate, the corresponding 2-chloro-3-nitro-5-(trifluoromethyl)benzoyl isothiocyanate (**2**) was reacted with piperidine. As illustrated, nucleophilic attack of the piperidine nitrogen atom at the isothiocyanate carbon atom leads to the anticipated 8-nitro-2-(piperidin-1-yl)-6-(trifluoromethyl)-1,3-benzothiazin-4-one (**3**). The alternative nucleophilic attack at the carbonyl carbon atom affords the side product (2-chloro-3-nitro-5-(trifluoromethyl)phenyl)(piperidin-1-yl)methanone (**4**), which was structurally characterized by X-ray crystallography in the present work. The ratio of **3** to **4** was found to vary depending on the reaction conditions. Temperatures at or below 283 K favour the formation of the anticipated **3**, whereas substantial amounts of **4** form at elevated temperatures (Rudolph, 2014). Since BTZs are in clinical development [see, for example, Makarov & Mikušová (2020) or Mariandyshv *et al.* (2020)], this observation is not only important for the improvement of synthetic yields but also for the compilation of known synthetic side products for drug quality control.

It is interesting to note that dinitrobenzamide derivatives related to **4** have been found to have some anti-mycobacterial activity (Christophe *et al.*, 2009; Trefzer *et al.*, 2010; Tiwari *et al.*, 2013), and the non-chlorinated analogue of **4** was reported to have anticoccidial activity (Welch *et al.*, 1969).

2. Structural commentary

Fig. 2 shows the molecular structure of **4** in the solid state. Selected geometric parameters are listed in Table 1. The dihedral angle between the plane of the nitro group and the mean plane of the benzene ring is $38.1(2)^\circ$, which can be attributed to the steric demand of the neighbouring chloro substituent at the benzene ring. The trifluoromethyl group

exhibits rotational disorder over two sites with 97.2(2)% occupancy for the major site. The plane of the amide group, as defined by C8, O3 and N2, is tilted out of the mean plane of the benzene ring by $79.6(1)^\circ$. The Winkler–Dunitz parameters for the amide linkage τ (twist angle) = 1.2° and χ_N (pyramidalization at nitrogen) = 4.0° indicate an almost planar amide group (Winkler & Dunitz, 1971). In the IR spectrum (see supporting information), the band at 1639 cm^{-1} can be assigned to the C=O stretching vibration of the amide group. The molecule is axially chiral, although the centrosymmetric crystal structure contains both enantiomers. The ^{13}C NMR spectrum of **4** in methanol- d_4 as well as chloroform- d at room temperature (see supporting information) displays five distinct signals in the aliphatic region, which are assigned to the piperidine carbon atoms, indicating that the rotation about the amide C–N bond is slow in solution under these conditions. The ^{13}C NMR chemical shift of the α -carbon atom C13 *syn* to

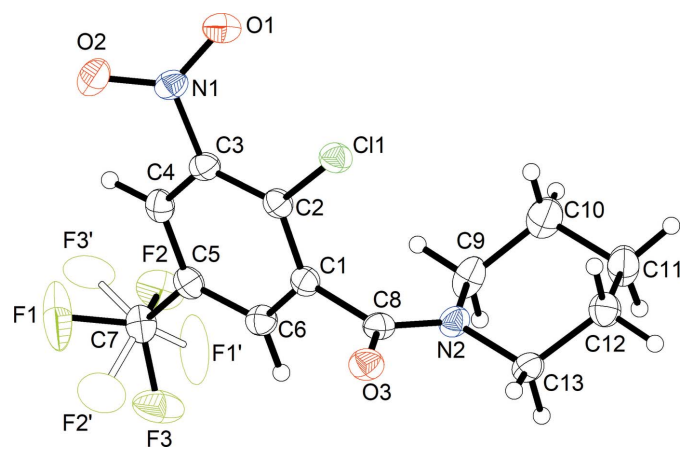


Figure 2

Molecular structure of **4**. Displacement ellipsoids are drawn at the 50% probability level. H atoms are represented by small spheres of arbitrary radii. The minor occupancy component of the disordered trifluoromethyl group is depicted by empty ellipsoids.

Table 1
Selected geometric parameters (Å, °).

C1—C8	1.510 (3)	C7—F3	1.328 (3)
C2—C11	1.725 (2)	C7—F2	1.336 (3)
C3—N1	1.468 (3)	C8—O3	1.234 (2)
C5—C7	1.497 (3)	C8—N2	1.342 (3)
C7—F1	1.325 (3)		
C4—C3—N1	116.41 (17)	N2—C9—C10	110.59 (18)
C2—C3—N1	122.35 (18)	C9—C10—C11	110.61 (19)
F1—C7—F3	107.69 (19)	C12—C11—C10	109.74 (18)
F1—C7—F2	105.98 (19)	C13—C12—C11	111.01 (18)
F3—C7—F2	105.59 (17)	N2—C13—C12	111.35 (17)
F1—C7—C5	112.43 (17)	O2—N1—O1	124.48 (17)
F3—C7—C5	112.80 (18)	O2—N1—C3	117.04 (17)
F2—C7—C5	111.86 (17)	O1—N1—C3	118.44 (16)
O3—C8—N2	124.72 (18)	C8—N2—C13	120.26 (16)
O3—C8—C1	118.43 (18)	C8—N2—C9	124.74 (16)
N2—C8—C1	116.85 (17)	C13—N2—C9	114.89 (16)
C4—C3—N1—O2	36.6 (2)	O3—C8—N2—C13	3.0 (3)
C2—C3—N1—O2	−143.29 (19)	C1—C8—N2—C13	−176.62 (17)
C4—C3—N1—O1	−141.34 (18)	O3—C8—N2—C9	179.0 (2)
C2—C3—N1—O1	38.8 (3)	C1—C8—N2—C9	−0.6 (3)

the carbonyl oxygen atom of the amide group is shielded compared with that of the *anti* α -carbon atom C9. In chloroform-*d*, the observed shielding magnitude of $\Delta\delta_C = 5.0$ ppm is within the range expected for a benzoylpiperidine (Rubiralta *et al.*, 1991). In the corresponding ^1H NMR spectrum, the *syn* protons with respect to the amide carbonyl oxygen atom are deshielded compared with those in the *anti* position ($\Delta\delta_H = 0.58$ ppm). Complete assignments of ^1H and ^{13}C NMR data in chloroform-*d* by ^{13}C , ^1H -HSQC and -HMBC NMR spectra can be found in the supporting information. Notably, the two separated methylene ^1H NMR signals assigned to C10 in chloroform-*d* appear as one signal in methanol-*d*₄.

In the solid state, the piperidine ring in **4** adopts a low-energy chair conformation with some minor angular deviations from ideal tetrahedral values, resulting from planarity at N2 due to involvement in the amide linkage. The puckering parameters of the piperidine six-membered ring, as calculated with *PLATON* (Spek, 2020), are $Q = 0.555$ (2) Å, $\theta = 4.1$ (2)° and $\varphi = 161$ (3)°. By way of comparison, the total puckering amplitude Q is 0.63 Å and the magnitude of distortion θ is 0° for an ideal cyclohexane chair (Cremer & Pople, 1975).

3. Supramolecular features

In general, the crystal structure of **4** appears to be dominated by close packing. According to Kitaigorodskii (1973), the space group *Pbca* is among those available for the densest packing of molecules of arbitrary shape. Nevertheless, the solid-state supramolecular structure features C—H...O contacts between an aromatic CH moiety and the amide oxygen atom of an adjacent molecule (Fig. 3*a*). The corresponding geometric parameters (Table 2) support the interpretation as a weak hydrogen bond (Thakuria *et al.*, 2017). These interactions link the molecules into strands extending by 2₁ screw symmetry in the [010] direction. The α -methylene groups of the piperidine ring, on which the amide group

Table 2
Hydrogen-bond geometry (Å, °).

<i>D</i> —H... <i>A</i>	<i>D</i> —H	H... <i>A</i>	<i>D</i> ... <i>A</i>	<i>D</i> —H... <i>A</i>
C6—H6...O3 ⁱ	0.95	2.59	3.526 (3)	169
C9—H9A...O1 ⁱⁱ	0.99	2.45	3.361 (3)	154
C9—H9B...O1 ⁱⁱⁱ	0.99	2.58	3.369 (3)	137
C13—H13A...Cg(C1—C6) ^{iv}	0.99	2.92	3.447 (2)	114

Symmetry codes: (i) $-x + 1, y + \frac{1}{2}, -z + \frac{1}{2}$; (ii) $-x + \frac{1}{2}, y + \frac{1}{2}, z$; (iii) $x, y + 1, z$; (iv) $x + \frac{3}{2}, -y + \frac{1}{2}, -z$.

should exert an electron-withdrawing effect, also form intermolecular C—H...O and C—H... π contacts, respectively, to the nitro group and the benzene ring of adjacent molecules (Fig. 3*b–d*). The corresponding geometric parameters (Table 2), however, reveal that these contacts may not have the same significance here as the aforementioned C_{aromatic}—H...O_{amide} short contact (Wood *et al.*, 2009). It is also worth noting that π — π stacking of the aromatic rings is not observed.

4. Database survey

A search of the Cambridge Structural Database (CSD; version 5.41 with March 2020 updates; Groom *et al.*, 2016) for related substituted *N*-benzoyl-piperidine compounds revealed about 30 structures, of which (2-chloro-3,5-dinitrophenyl)(piperidin-1-yl)methanone (CSD refcode: URALIJ; Luo *et al.*, 2011) is structurally most related to **4**. Similar to **4**, the 3-nitro group with the neighbouring chloro substituent is tilted out of the mean plane of the benzene ring by 36.2°. At 75.8°, the dihedral angle between the amide plane and the mean plane of the benzene ring is comparable with that in **4**. Likewise, the

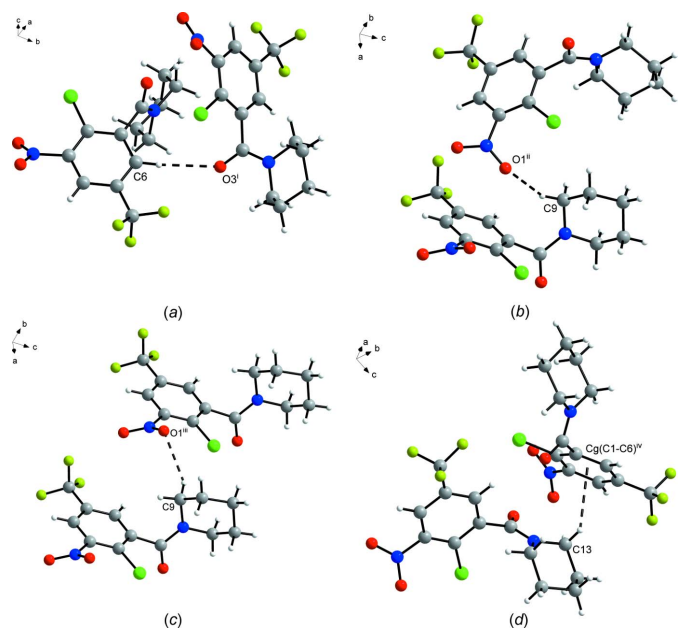


Figure 3
Short contacts (dashed lines) between adjacent molecules in the crystal structure of **4**. The minor component of the disordered trifluoromethyl group is omitted for clarity. Symmetry codes: (i) $-x + 1, y + \frac{1}{2}, -z + \frac{1}{2}$; (ii) $-x + \frac{1}{2}, y + \frac{1}{2}, z$; (iii) $x, y + 1, z$; (iv) $x + \frac{3}{2}, -y + \frac{1}{2}, -z$.

piperidine ring exhibits a chair conformation with a planar structure at the nitrogen atom. In contrast to **4**, the solid-state supramolecular structure of URALIJ exhibits π - π stacking of the aromatic rings. Interestingly, a CSD search for the 2-chloro-3-nitro-5-(trifluoromethyl)phenyl moiety present in **4** led to only one structure, *viz.* 2-chloro-1,3-dinitro-5-(trifluoromethyl)benzene (JIHNUM; del Casino *et al.*, 2018), also known as chloralin, which is active against *Plasmodium*, but which also shows toxicity in mice.

5. Anti-mycobacterial evaluation

The anti-mycobacterial activity of **4** was evaluated against *Mycobacterium smegmatis* mc² 155 and *Mycobacterium abscessus* ATCC19977, using broth microdilution assays [for the assay protocols, see the supporting information and Richter, Strauch *et al.* (2018)]. For both mycobacterial species, no growth inhibition was detectable up to a concentration of 100 μ M. For *M. smegmatis*, the findings are consistent with the activity data for a related nitrobenzamide derivative reported by Tiwari *et al.* (2013). CT319, a 3-nitro-5-(trifluoromethyl)benzamide derivative, however, showed activity against *M. smegmatis* mc² 155 and other mycobacterial strains (Trefzer *et al.*, 2010).

6. Synthesis and crystallization

Chemicals were purchased and used as received. The synthesis of **1** is described elsewhere (Welch *et al.*, 1969). Solvents were of reagent grade and were distilled before use. The IR spectrum was measured on a Bruker TENSOR II FT-IR spectrometer at a resolution of 4 cm^{-1} . NMR spectra were recorded at room temperature on an Agilent Technologies VNMRs 400 MHz NMR spectrometer (abbreviations: *d* = doublet, *q* = quartet, *m* = multiplet). Chemical shifts are referenced to the residual signals of methanol-*d*₄ (δ_{H} = 3.35 ppm, δ_{C} = 49.3 ppm) or chloroform-*d* (δ_{H} = 7.26 ppm, δ_{C} = 77.2 ppm).

2.7 mL (37.0 mmol) of SOCl_2 were added to a stirred solution of **1** (5.00 g, 18.5 mmol) in toluene, and the mixture was heated to reflux for two h. The solvent was subsequently removed under reduced pressure, and the acid chloride thus obtained was used without purification. The residue was taken up in 6.5 mL of acetonitrile and a solution of 1.41 g (18.5 mmol) NH_4SCN in 55 mL of acetonitrile was added dropwise with stirring to obtain **2** *in situ*. After stirring for 5 min at 313 K, the resulting NH_4Cl precipitate was filtered off, and 3.7 mL (37.0 mmol) of piperidine were added. The mixture was refluxed overnight, and then the solvent was removed under reduced pressure. Water was added to the residue and, after extraction with dichloromethane, the organic phase was washed with 10% aqueous NaHCO_3 and dried over MgSO_4 . After removal of the solvent, the crude product was subjected to flash chromatography on silica gel, eluting with ethyl acetate/*n*-heptane (gradient 10–50% *v/v*), to isolate 1.09 g (3.0 mmol, 16%) of **3** and a minor amount of the side product **4**. ¹H and ¹³C NMR spectroscopic and mass

Table 3
Experimental details.

Crystal data	
Chemical formula	$\text{C}_{13}\text{H}_{12}\text{ClF}_3\text{N}_2\text{O}_3$
M_r	336.70
Crystal system, space group	Orthorhombic, <i>Pbca</i>
Temperature (K)	100
a, b, c (Å)	18.0904 (7), 7.8971 (3), 19.8043 (8)
V (Å ³)	2829.28 (19)
Z	8
Radiation type	Cu $K\alpha$
μ (mm ⁻¹)	2.88
Crystal size (mm)	0.59 × 0.50 × 0.44
Data collection	
Diffractometer	Bruker Kappa Mach3 APEXII
Absorption correction	Gaussian (<i>SADABS</i> ; Krause <i>et al.</i> , 2015)
$T_{\text{min}}, T_{\text{max}}$	0.297, 0.586
No. of measured, independent and observed [$I > 2\sigma(I)$] reflections	49954, 2784, 2699
R_{int}	0.041
$(\sin \theta/\lambda)_{\text{max}}$ (Å ⁻¹)	0.617
Refinement	
$R[F^2 > 2\sigma(F^2)], wR(F^2), S$	0.043, 0.115, 1.15
No. of reflections	2784
No. of parameters	209
No. of restraints	45
H-atom treatment	H-atom parameters constrained
$\Delta\rho_{\text{max}}, \Delta\rho_{\text{min}}$ (e Å ⁻³)	0.32, -0.32

Computer programs: *APEX3* (Bruker, 2017), *SAINT* (Bruker, 2004), *SHELXT2014/4* (Sheldrick, 2015a), *SHELXL2018/3* (Sheldrick, 2015b), *DIAMOND* (Brandenburg, 2018), *enCIFer* (Allen *et al.*, 2004) and *publCIF* (Westrip, 2010).

spectrometric data of **3** were in agreement with those in the literature (Rudolph, 2014; Rudolph *et al.*, 2016). Crystals of **4** suitable for X-ray crystallography were obtained from a solution in ethyl acetate/heptane (1:1) by slow evaporation of the solvents at room temperature. NMR spectroscopic data for **4**:

¹H NMR (400 MHz, CD_3OD) δ 8.42 (*d*, ⁴ $J_{\text{meta}} = 2.2$ Hz, 1H, Ar-*H*), 8.09 (*d*, ⁴ $J_{\text{meta}} = 2.2$ Hz, 1H, Ar-*H*), 3.88–3.71 (*m*, 2H, N- CH_2), 3.33–3.21 (*m*, 2H, N- CH_2), 1.76 (*m*, 4H, CH_2), 1.64 (*m*, 2H, CH_2) ppm; ¹³C NMR (101 MHz, CD_3OD) δ 165.5, 150.7, 141.8, 132.3 (*q*, ² $J_{\text{C,F}} = 35$ Hz), 129.2 (*q*, ³ $J_{\text{C,F}} = 4$ Hz), 128.1, 124.4 (*q*, ³ $J_{\text{C,F}} = 4$ Hz), 124.1 (*q*, ¹ $J_{\text{C,F}} = 273$ Hz), 49.5, 44.3, 27.6, 26.7, 25.5 ppm.

¹H NMR (400 MHz, CDCl_3) δ 8.07 (*d*, ⁴ $J_{\text{meta}} = 2.0$ Hz, 1H, C4-*H*), 7.73 (*d*, ⁴ $J_{\text{meta}} = 2.0$ Hz, 1H, C6-*H*), 3.83–3.68 (*m*, 2H, C13- CH_2), 3.22 (*ddd*, ² $J_{\text{gem}} = 13.2$ Hz, ³ $J_{\text{vic}} = 7.1$, 4.0 Hz, 1H, C9- CH_2), 3.15 (*ddd*, ² $J_{\text{gem}} = 13.2$ Hz, ³ $J_{\text{vic}} = 7.1$, 4.0 Hz, 1H, C9- CH_2), 1.70 (*m*, 4H, C11, C12- CH_2), 1.65–1.57 (*m*, 1H, C10- CH_2), 1.56–1.47 (*m*, 1H, C10- CH_2) ppm; ¹³C NMR (101 MHz, CDCl_3) δ 163.5 (C8, C=O), 148.9 (C3), 141.1 (C1), 131.2 (*q*, ² $J_{\text{C,F}} = 35$ Hz, C5), 127.8 (*q*, ³ $J_{\text{C,F}} = 4$ Hz, C6), 127.6 (C2), 122.7 (*q*, ³ $J_{\text{C,F}} = 4$ Hz, C4), 122.4 (*q*, ¹ $J_{\text{C,F}} = 273$ Hz, C7), 48.3 (C9), 43.3 (C13), 26.7 (C10), 25.7 (C12), 24.6 (C11) ppm.

7. Refinement

Crystal data, data collection and structure refinement details are summarized in Table 3. The rotational disorder of the trifluoromethyl group was refined using a split model with

similar distance restraints on the 1,2- and 1,3-distances and equal atomic displacement parameters for opposite fluorine atoms belonging to different disorder sites. Refinement of the ratio of occupancies by means of a free variable resulted in 0.972 (2):0.028 (2). Hydrogen-atom positions were calculated geometrically with $C_a-H = 0.95 \text{ \AA}$ and $C_m-H = 0.99 \text{ \AA}$ ($a =$ aromatic and $m =$ methylene), and refined with the appropriate riding model and $U_{iso}(H) = 1.2 U_{eq}(C)$.

Acknowledgements

We thank Professor Christian W. Lehmann for providing access to the X-ray diffraction facility and Heike Schucht for technical assistance.

Funding information

We acknowledge the financial support within the funding programme Open Access Publishing by the German Research Foundation (DFG).

References

- Allen, F. H., Johnson, O., Shields, G. P., Smith, B. R. & Towler, M. (2004). *J. Appl. Cryst.* **37**, 335–338.
- Brandenburg, K. (2018). *DIAMOND*. Crystal Impact GbR, Bonn, Germany.
- Bruker (2004). *SAINT*. Bruker AXS Inc., Madison, Wisconsin, USA.
- Bruker (2017). *APEX3*. Bruker AXS Inc., Madison, Wisconsin, USA.
- Casino, A. del, Lukinović, V., Bhatt, R., Randle, L. E., Dascombe, M. J., Fennell, B. J., Drew, M. G. B., Bell, A., Fielding, A. J. & Ismail, F. M. D. (2018). *ChemistrySelect* **3**, 7572–7580.
- Christophe, T., Jackson, M., Jeon, H. K., Fenistein, D., Contreras-Dominguez, M., Kim, J., Genovesio, A., Carralot, J.-P., Ewann, F., Kim, E. H., Lee, S. Y., Kang, S., Seo, M. J., Park, E. J., Škovierová, H., Pham, H., Riccardi, G., Nam, J. Y., Marsollier, L., Kempf, M., Joly-Guillou, M.-L., Oh, T., Shin, W. K., No, Z., Nehrbass, U., Brosch, R., Cole, S. T. & Brodin, P. (2009). *PLoS Pathog.* **5**, e1000645.
- Cremer, D. & Pople, J. A. (1975). *J. Am. Chem. Soc.* **97**, 1354–1358.
- Groom, C. R., Bruno, I. J., Lightfoot, M. P. & Ward, S. C. (2016). *Acta Cryst.* **B72**, 171–179.
- Kitaigorodskii, A. I. (1973). *Molecular Crystals and Molecules*. London: Academic Press.
- Krause, L., Herbst-Irmer, R., Sheldrick, G. M. & Stalke, D. (2015). *J. Appl. Cryst.* **48**, 3–10.
- Luo, X., Huang, Y.-C., Gao, C. & Yu, L.-T. (2011). *Acta Cryst.* **E67**, o1066.
- Makarov, V. (2011). *PCT Int. Appl.* WO 2011132070 A1.
- Makarov, V., Cole, S. T. & Moellmann, U. (2007). *PCT Int. Appl.* WO 2007134625 A1.
- Makarov, V. & Mikušová, K. (2020). *Appl. Sci.* **10**, 2269.
- Mariandyshev, A. O., Khokhlov, A. L., Smerdin, S. V., Shcherbakova, V. S., Igumnova, O. V., Ozerova, I. V., Bolgarina, A. A. & Nikitina, N. A. (2020). *Ter. Arkh.* **92**, 61–72.
- Mikušová, K., Makarov, V. & Neres, J. (2014). *Curr. Pharm. Des.* **20**, 4379–4403.
- Moellmann, U., Makarov, V. & Cole, S. T. (2009). *PCT Int. Appl.* WO 2009010163 A1.
- Richter, A., Rudolph, I., Möllmann, U., Voigt, K., Chung, C., Singh, O. M. P., Rees, M., Mendoza-Losana, A., Bates, R., Ballell, L., Batt, S., Veerapen, N., Fütterer, K., Besra, G., Imming, P. & Argyrou, A. (2018). *Sci. Rep.* **8**, 13473.
- Richter, A., Strauch, A., Chao, J., Ko, M. & Av-Gay, Y. (2018). *Antimicrob. Agents Chemother.* **62**, e00828–18.
- Rubiralta, M., Giralt, E. & Diez, A. (1991). 7 - *N-Acylpiperidines. A Useful Tool for Stereocontrol in Organic Synthesis*. In: *Studies in Organic Chemistry*, vol. 43, pp. 193–224. Amsterdam: Elsevier.
- Rudolph, A. I. (2014). PhD thesis, Martin-Luther-Universität Halle-Wittenberg, Halle (Saale), Germany.
- Rudolph, I., Imming, P. & Richter, A. (2016). *Ger. Offen.* DE 102014012546 A1 20160331.
- Sheldrick, G. M. (2015a). *Acta Cryst.* **A71**, 3–8.
- Sheldrick, G. M. (2015b). *Acta Cryst.* **C71**, 3–8.
- Spek, A. L. (2020). *Acta Cryst.* **E76**, 1–11.
- Thakuria, R., Sarma, B. & Nangia, A. (2017). *Hydrogen Bonding in Molecular Crystals*. In: *Comprehensive Supramolecular Chemistry II*, vol. 7, edited by J. L. Atwood, pp. 25–48. Oxford: Elsevier.
- Tiwari, R., Moraski, G. C., Krchňák, V., Miller, P. A., Colon-Martinez, M., Herrero, E., Oliver, A. G. & Miller, M. J. (2013). *J. Am. Chem. Soc.* **135**, 3539–3549.
- Trefzer, C., Rengifo-Gonzalez, M., Hinner, M. J., Schneider, P., Makarov, V., Cole, S. T. & Johnsson, K. (2010). *J. Am. Chem. Soc.* **132**, 13663–13665.
- Welch, D. E., Baron, R. R. & Burton, B. A. (1969). *J. Med. Chem.* **12**, 299–303.
- Westrip, S. P. (2010). *J. Appl. Cryst.* **43**, 920–925.
- Winkler, F. K. & Dunitz, J. D. (1971). *J. Mol. Biol.* **59**, 169–182.
- Wood, P. A., Allen, F. H. & Pidcock, E. (2009). *CrystEngComm*, **11**, 1563–1571.
- Zhang, G. & Aldrich, C. C. (2019). *Acta Cryst.* **C75**, 1031–1035.

supporting information

Acta Cryst. (2020). E76, 1442-1446 [https://doi.org/10.1107/S2056989020010658]

[2-Chloro-3-nitro-5-(trifluoromethyl)phenyl](piperidin-1-yl)methanone: structural characterization of a side product in benzothiazinone synthesis

Tamira Eckhardt, Richard Goddard, Ines Rudolph, Adrian Richter, Christoph Lehmann, Peter Imming and Rüdiger W. Seidel

Computing details

Data collection: *APEX3* (Bruker, 2017); cell refinement: *S SAINT* (Bruker, 2004); data reduction: *S SAINT* (Bruker, 2004); program(s) used to solve structure: *SHELXT2014/4* (Sheldrick, 2015a); program(s) used to refine structure: *SHELXL2018/3* (Sheldrick, 2015b); molecular graphics: *DIAMOND* (Brandenburg, 2018); software used to prepare material for publication: *enCIFer* (Allen *et al.*, 2004) and *publCIF* (Westrip, 2010).

[2-Chloro-3-nitro-5-(trifluoromethyl)phenyl](piperidin-1-yl)methanone

Crystal data

$C_{13}H_{12}ClF_3N_2O_3$

$M_r = 336.70$

Orthorhombic, *Pbca*

$a = 18.0904$ (7) Å

$b = 7.8971$ (3) Å

$c = 19.8043$ (8) Å

$V = 2829.28$ (19) Å³

$Z = 8$

$F(000) = 1376$

$D_x = 1.581$ Mg m⁻³

Cu *Kα* radiation, $\lambda = 1.54178$ Å

Cell parameters from 9968 reflections

$\theta = 4.9$ – 71.6°

$\mu = 2.88$ mm⁻¹

$T = 100$ K

Block, colourless

$0.59 \times 0.50 \times 0.44$ mm

Data collection

Bruker Kappa Mach3 APEXII

diffractometer

Radiation source: 0.2×2 mm² focus rotating

anode

MONTEL graded multilayer optics

monochromator

Detector resolution: 66.67 pixels mm⁻¹

φ - and ω -scans

Absorption correction: gaussian

(SADABS; Krause *et al.*, 2015)

$T_{\min} = 0.297$, $T_{\max} = 0.586$

49954 measured reflections

2784 independent reflections

2699 reflections with $I > 2\sigma(I)$

$R_{\text{int}} = 0.041$

$\theta_{\max} = 72.2^\circ$, $\theta_{\min} = 4.9^\circ$

$h = -21 \rightarrow 22$

$k = -9 \rightarrow 9$

$l = -24 \rightarrow 24$

Refinement

Refinement on F^2

Least-squares matrix: full

$R[F^2 > 2\sigma(F^2)] = 0.043$

$wR(F^2) = 0.115$

$S = 1.15$

2784 reflections

209 parameters

45 restraints

Primary atom site location: dual

Secondary atom site location: difference Fourier map

Hydrogen site location: inferred from neighbouring sites

H-atom parameters constrained

$$w = 1/[\sigma^2(F_o^2) + (0.0508P)^2 + 2.7994P]$$

where $P = (F_o^2 + 2F_c^2)/3$
 $(\Delta/\sigma)_{\max} < 0.001$

$$\Delta\rho_{\max} = 0.32 \text{ e } \text{\AA}^{-3}$$

$$\Delta\rho_{\min} = -0.32 \text{ e } \text{\AA}^{-3}$$

Special details

Geometry. All esds (except the esd in the dihedral angle between two l.s. planes) are estimated using the full covariance matrix. The cell esds are taken into account individually in the estimation of esds in distances, angles and torsion angles; correlations between esds in cell parameters are only used when they are defined by crystal symmetry. An approximate (isotropic) treatment of cell esds is used for estimating esds involving l.s. planes.

Fractional atomic coordinates and isotropic or equivalent isotropic displacement parameters (\AA^2)

	<i>x</i>	<i>y</i>	<i>z</i>	$U_{\text{iso}}^*/U_{\text{eq}}$	Occ. (<1)
C1	0.41556 (10)	0.3250 (3)	0.23581 (10)	0.0230 (4)	
C2	0.38370 (10)	0.1651 (3)	0.23833 (10)	0.0224 (4)	
C3	0.35007 (10)	0.1004 (3)	0.18023 (10)	0.0227 (4)	
C4	0.34763 (10)	0.1927 (3)	0.12111 (10)	0.0243 (4)	
H4	0.325215	0.146458	0.081847	0.029*	
C5	0.37831 (10)	0.3541 (3)	0.11961 (10)	0.0242 (4)	
C6	0.41190 (11)	0.4206 (3)	0.17666 (10)	0.0250 (4)	
H6	0.432417	0.531321	0.175487	0.030*	
C7	0.37425 (12)	0.4549 (3)	0.05572 (11)	0.0298 (5)	
C8	0.45848 (10)	0.3906 (2)	0.29575 (10)	0.0232 (4)	
C9	0.34929 (13)	0.5683 (3)	0.32422 (11)	0.0327 (5)	
H9A	0.325497	0.503425	0.287381	0.039*	
H9B	0.351745	0.688568	0.310277	0.039*	
C10	0.30335 (12)	0.5528 (3)	0.38813 (13)	0.0404 (6)	
H10A	0.296350	0.431647	0.399304	0.048*	
H10B	0.254021	0.603627	0.380559	0.048*	
C11	0.34134 (13)	0.6421 (3)	0.44689 (11)	0.0373 (5)	
H11A	0.344826	0.764952	0.437412	0.045*	
H11B	0.311898	0.626777	0.488581	0.045*	
C12	0.41843 (12)	0.5691 (3)	0.45695 (10)	0.0294 (5)	
H12A	0.443955	0.632047	0.493365	0.035*	
H12B	0.414464	0.449164	0.470978	0.035*	
C13	0.46343 (11)	0.5807 (3)	0.39245 (10)	0.0277 (4)	
H13A	0.473754	0.701122	0.382205	0.033*	
H13B	0.511333	0.522352	0.398982	0.033*	
N1	0.31581 (9)	-0.0681 (2)	0.17845 (9)	0.0253 (4)	
N2	0.42423 (9)	0.5038 (2)	0.33544 (8)	0.0249 (4)	
O1	0.28104 (8)	-0.1161 (2)	0.22819 (8)	0.0324 (4)	
O2	0.32229 (8)	-0.1493 (2)	0.12611 (8)	0.0341 (4)	
O3	0.52198 (7)	0.33806 (19)	0.30471 (7)	0.0288 (3)	
F1	0.38438 (14)	0.3603 (2)	0.00122 (7)	0.0711 (7)	0.972 (2)
F2	0.30831 (8)	0.52847 (19)	0.04797 (8)	0.0418 (4)	0.972 (2)
F3	0.42321 (8)	0.5801 (2)	0.05379 (8)	0.0470 (4)	0.972 (2)
F1'	0.352 (3)	0.612 (3)	0.0688 (18)	0.0711 (7)	0.028 (2)
F2'	0.4387 (11)	0.472 (6)	0.0269 (18)	0.0418 (4)	0.028 (2)
F3'	0.325 (2)	0.397 (5)	0.0129 (15)	0.0470 (4)	0.028 (2)

C11 0.38924 (3) 0.05417 (6) 0.31320 (2) 0.02635 (16)

Atomic displacement parameters (Å²)

	U^{11}	U^{22}	U^{33}	U^{12}	U^{13}	U^{23}
C1	0.0194 (9)	0.0250 (9)	0.0246 (9)	0.0021 (7)	0.0012 (7)	-0.0019 (8)
C2	0.0186 (8)	0.0246 (9)	0.0239 (9)	0.0021 (7)	0.0011 (7)	0.0002 (8)
C3	0.0166 (8)	0.0219 (9)	0.0296 (10)	0.0011 (7)	0.0009 (7)	-0.0021 (8)
C4	0.0202 (9)	0.0288 (10)	0.0239 (9)	0.0050 (8)	-0.0004 (7)	-0.0031 (8)
C5	0.0219 (9)	0.0261 (10)	0.0247 (10)	0.0056 (8)	0.0021 (7)	0.0011 (8)
C6	0.0248 (10)	0.0226 (9)	0.0277 (10)	0.0006 (8)	0.0004 (8)	0.0002 (8)
C7	0.0350 (11)	0.0292 (11)	0.0251 (10)	0.0056 (9)	0.0005 (8)	-0.0002 (8)
C8	0.0225 (9)	0.0226 (9)	0.0245 (9)	-0.0035 (8)	-0.0003 (7)	0.0033 (8)
C9	0.0335 (11)	0.0298 (11)	0.0347 (11)	0.0094 (9)	-0.0117 (9)	-0.0088 (9)
C10	0.0200 (10)	0.0517 (15)	0.0495 (14)	0.0058 (9)	-0.0038 (9)	-0.0188 (11)
C11	0.0324 (11)	0.0474 (14)	0.0322 (11)	0.0039 (10)	-0.0011 (9)	-0.0114 (10)
C12	0.0308 (11)	0.0327 (11)	0.0247 (10)	-0.0010 (9)	-0.0013 (8)	0.0002 (8)
C13	0.0267 (10)	0.0306 (10)	0.0257 (10)	-0.0070 (8)	-0.0028 (8)	-0.0018 (8)
N1	0.0190 (8)	0.0260 (9)	0.0310 (9)	-0.0009 (6)	-0.0037 (7)	-0.0016 (7)
N2	0.0213 (8)	0.0277 (9)	0.0257 (8)	-0.0010 (7)	-0.0042 (7)	-0.0030 (7)
O1	0.0267 (7)	0.0334 (8)	0.0371 (8)	-0.0062 (6)	0.0010 (6)	0.0028 (7)
O2	0.0348 (8)	0.0320 (8)	0.0356 (8)	-0.0010 (6)	-0.0045 (6)	-0.0098 (7)
O3	0.0204 (7)	0.0324 (8)	0.0337 (8)	0.0005 (6)	-0.0017 (6)	-0.0003 (6)
F1	0.151 (2)	0.0382 (9)	0.0239 (7)	0.0278 (10)	0.0154 (9)	-0.0002 (6)
F2	0.0336 (7)	0.0457 (8)	0.0460 (8)	0.0053 (6)	-0.0056 (6)	0.0175 (7)
F3	0.0389 (8)	0.0567 (10)	0.0453 (8)	-0.0142 (7)	-0.0052 (6)	0.0251 (7)
F1'	0.151 (2)	0.0382 (9)	0.0239 (7)	0.0278 (10)	0.0154 (9)	-0.0002 (6)
F2'	0.0336 (7)	0.0457 (8)	0.0460 (8)	0.0053 (6)	-0.0056 (6)	0.0175 (7)
F3'	0.0389 (8)	0.0567 (10)	0.0453 (8)	-0.0142 (7)	-0.0052 (6)	0.0251 (7)
C11	0.0267 (3)	0.0273 (3)	0.0250 (3)	-0.00271 (18)	0.00002 (17)	0.00364 (17)

Geometric parameters (Å, °)

C1—C2	1.389 (3)	C8—N2	1.342 (3)
C1—C6	1.395 (3)	C9—N2	1.465 (3)
C1—C8	1.510 (3)	C9—C10	1.519 (3)
C2—C3	1.398 (3)	C9—H9A	0.9900
C2—C11	1.725 (2)	C9—H9B	0.9900
C3—C4	1.380 (3)	C10—C11	1.525 (3)
C3—N1	1.468 (3)	C10—H10A	0.9900
C4—C5	1.390 (3)	C10—H10B	0.9900
C4—H4	0.9500	C11—C12	1.522 (3)
C5—C6	1.386 (3)	C11—H11A	0.9900
C5—C7	1.497 (3)	C11—H11B	0.9900
C6—H6	0.9500	C12—C13	1.518 (3)
C7—F2'	1.304 (14)	C12—H12A	0.9900
C7—F3'	1.314 (14)	C12—H12B	0.9900
C7—F1	1.325 (3)	C13—N2	1.465 (2)

C7—F3	1.328 (3)	C13—H13A	0.9900
C7—F1'	1.332 (14)	C13—H13B	0.9900
C7—F2	1.336 (3)	N1—O2	1.225 (2)
C8—O3	1.234 (2)	N1—O1	1.229 (2)
C2—C1—C6	120.16 (18)	C10—C9—H9A	109.5
C2—C1—C8	119.82 (17)	N2—C9—H9B	109.5
C6—C1—C8	119.90 (17)	C10—C9—H9B	109.5
C1—C2—C3	118.92 (18)	H9A—C9—H9B	108.1
C1—C2—C11	117.93 (15)	C9—C10—C11	110.61 (19)
C3—C2—C11	123.13 (16)	C9—C10—H10A	109.5
C4—C3—C2	121.24 (18)	C11—C10—H10A	109.5
C4—C3—N1	116.41 (17)	C9—C10—H10B	109.5
C2—C3—N1	122.35 (18)	C11—C10—H10B	109.5
C3—C4—C5	119.32 (18)	H10A—C10—H10B	108.1
C3—C4—H4	120.3	C12—C11—C10	109.74 (18)
C5—C4—H4	120.3	C12—C11—H11A	109.7
C6—C5—C4	120.33 (18)	C10—C11—H11A	109.7
C6—C5—C7	120.58 (19)	C12—C11—H11B	109.7
C4—C5—C7	119.09 (18)	C10—C11—H11B	109.7
C5—C6—C1	119.98 (19)	H11A—C11—H11B	108.2
C5—C6—H6	120.0	C13—C12—C11	111.01 (18)
C1—C6—H6	120.0	C13—C12—H12A	109.4
F2'—C7—F3'	111.1 (19)	C11—C12—H12A	109.4
F1—C7—F3	107.69 (19)	C13—C12—H12B	109.4
F2'—C7—F1'	105.2 (19)	C11—C12—H12B	109.4
F3'—C7—F1'	104.0 (19)	H12A—C12—H12B	108.0
F1—C7—F2	105.98 (19)	N2—C13—C12	111.35 (17)
F3—C7—F2	105.59 (17)	N2—C13—H13A	109.4
F2'—C7—C5	112.3 (15)	C12—C13—H13A	109.4
F3'—C7—C5	113.2 (15)	N2—C13—H13B	109.4
F1—C7—C5	112.43 (17)	C12—C13—H13B	109.4
F3—C7—C5	112.80 (18)	H13A—C13—H13B	108.0
F1'—C7—C5	110.3 (15)	O2—N1—O1	124.48 (17)
F2—C7—C5	111.86 (17)	O2—N1—C3	117.04 (17)
O3—C8—N2	124.72 (18)	O1—N1—C3	118.44 (16)
O3—C8—C1	118.43 (18)	C8—N2—C13	120.26 (16)
N2—C8—C1	116.85 (17)	C8—N2—C9	124.74 (16)
N2—C9—C10	110.59 (18)	C13—N2—C9	114.89 (16)
N2—C9—H9A	109.5		
C6—C1—C2—C3	1.9 (3)	C6—C5—C7—F1'	-47 (3)
C8—C1—C2—C3	-174.16 (17)	C4—C5—C7—F1'	133 (3)
C6—C1—C2—C11	-179.32 (15)	C6—C5—C7—F2	-99.4 (2)
C8—C1—C2—C11	4.6 (2)	C4—C5—C7—F2	80.3 (2)
C1—C2—C3—C4	-0.5 (3)	C2—C1—C8—O3	77.8 (2)
C11—C2—C3—C4	-179.22 (14)	C6—C1—C8—O3	-98.3 (2)
C1—C2—C3—N1	179.37 (16)	C2—C1—C8—N2	-102.6 (2)

C11—C2—C3—N1	0.6 (3)	C6—C1—C8—N2	81.4 (2)
C2—C3—C4—C5	-0.9 (3)	N2—C9—C10—C11	55.5 (3)
N1—C3—C4—C5	179.25 (16)	C9—C10—C11—C12	-56.9 (3)
C3—C4—C5—C6	0.9 (3)	C10—C11—C12—C13	55.8 (3)
C3—C4—C5—C7	-178.87 (18)	C11—C12—C13—N2	-53.4 (2)
C4—C5—C6—C1	0.5 (3)	C4—C3—N1—O2	36.6 (2)
C7—C5—C6—C1	-179.75 (18)	C2—C3—N1—O2	-143.29 (19)
C2—C1—C6—C5	-1.9 (3)	C4—C3—N1—O1	-141.34 (18)
C8—C1—C6—C5	174.13 (18)	C2—C3—N1—O1	38.8 (3)
C6—C5—C7—F2'	70 (2)	O3—C8—N2—C13	3.0 (3)
C4—C5—C7—F2'	-110 (2)	C1—C8—N2—C13	-176.62 (17)
C6—C5—C7—F3'	-163 (2)	O3—C8—N2—C9	179.0 (2)
C4—C5—C7—F3'	17 (2)	C1—C8—N2—C9	-0.6 (3)
C6—C5—C7—F1	141.5 (2)	C12—C13—N2—C8	-130.0 (2)
C4—C5—C7—F1	-38.8 (3)	C12—C13—N2—C9	53.6 (2)
C6—C5—C7—F3	19.5 (3)	C10—C9—N2—C8	129.2 (2)
C4—C5—C7—F3	-160.82 (18)	C10—C9—N2—C13	-54.6 (2)

Hydrogen-bond geometry (Å, °)

<i>D</i> —H... <i>A</i>	<i>D</i> —H	H... <i>A</i>	<i>D</i> ... <i>A</i>	<i>D</i> —H... <i>A</i>
C6—H6...O3 ⁱ	0.95	2.59	3.526 (3)	169
C9—H9 <i>A</i> ...O1 ⁱⁱ	0.99	2.45	3.361 (3)	154
C9—H9 <i>B</i> ...O1 ⁱⁱⁱ	0.99	2.58	3.369 (3)	137
C13—H13 <i>A</i> ...Cg(C1—C6) ^{iv}	0.99	2.92	3.447 (2)	114

Symmetry codes: (i) $-x+1, y+1/2, -z+1/2$; (ii) $-x+1/2, y+1/2, z$; (iii) $x, y+1, z$; (iv) $x+3/2, -y+1/2, -z$.